JOURNAL OF MATERIALS SCIENCE 24 (1989) 2794–2800

The synthesis of carbides by carbothermic reduction of mineral oxides in a d.c. transferred arc plasma

J. J. MOORE
Department of Chemical and Materials Engineering, University of Auckland, New Zealand

The carbothermic reduction of commercially available mineral concentrates of magnetite and chromite has been investigated using a 70 kW d.c. transferred arc plasma system. The degree of metallization achieved is discussed with respect to the presence of slag forming constituents present in the mineral, particle size, thermodynamics and kinetics. The products were characterized using optical, electron and Auger microscopy techniques and the degree of metastability evaluated.

1. Introduction

Considerable advantages can be gained by utilizing the plasma medium as a reaction medium for the synthesis of high temperature materials. The introduction of a thoroughly mixed feed of mineral oxide and graphite powder into a plasma has potential as a low volume–high throughput reactor system in which the reactants dissociate and ionize within the high temperature fields present within the plasma medium. Such highly reactive species are capable of enhanced reaction kinetics enabling a substantial degree of reduction of the mineral oxides to be achieved in less than 100 msec. Since the products, on leaving the plasma, rapidly transform from a liquid to a solid condition the rate of cooling can be significant enabling high metastability to be achieved with respect to both carbon saturation and fineness of structure of the resulting carbide. This paper discusses the reduction of commercially available mineral concentrates of magnetite and chromite using a graphite reductant in a 70 kW d.c. transferred arc plasma.

2. Experimental procedure

The plasma reactor (Fig. 1), comprised a hollow graphite cathode electrode and a ring graphite anode, was constructed such that the arc being transferred to the anode was made to orbit around the ring anode by electromagnetic means. A full description of this plasma system was given in an earlier paper [1]. This provided an increased volume of plasma and, therefore, an increased reaction volume. The concentrate–graphite mixtures were transported from a vibratory feeder into the reactor and allowed to fall, under gravity, at an angle into the top of the plasma cone adjacent to the hollow cathode as indicated in Fig. 1. The products from the plasma medium were simply quenched in air in a free fall system and collected in a crucible. Argon was used as the plasma gas which was passed through the hollow graphite electrode at approximately $0.8\,m^3\,h^{-1}$.

The products were metallographically examined using optical microscopy and scanning electron microscopy (SEM) and analysed chemically using an energy dispersive X-ray (EDAX) facility on the SEM and internally set standards on the scanning Auger microprobe, (SAM).

3. Thermodynamic and kinetic considerations

The thermodynamic and kinetic considerations for carbothermic reduction of minerals in a d.c. plasma environment have already been discussed [2]. The conclusions from this discussion were that, for metal oxides more stable than Fe_3O_4, there is a greater tendency to produce the carbide rather than elemental metal as shown in the $\Delta G°–T$ diagram, Fig. 2. The data presented in Fig. 2 indicate that the tendency to form iron or Fe_3C from carbothermic reduction of Fe_3O_4 is approximately equal. However, as temperatures exceed 1200° C, the tendency to produce carbides of chromium rather than elemental chromium increases.

The conclusions from the kinetic considerations were that the gasification of carbon is the rate controlling step as it is in conventional gas–solid reduction processes at lower temperatures [3–7], for example 1000° C. Therefore, the controlling reaction is the Boudouard reaction i.e. $CO_2 + C = 2CO$. Also, from earlier observations [2] of plasma reduction of iron oxide, there appeared to be an optimum amount of oxygen needed within the plasma environment in order to produce CO_2 which would enable the Boudouard reaction to proceed effectively.

4. Experimental results

The chemical analysis and size distribution of magnetite and chromite concentrates used in this investigation are given in Tables I and II. These two concentrates were chosen since they would produce essentially a carbon saturated metallic iron from the

0022–2461/89 $03.00 + .12

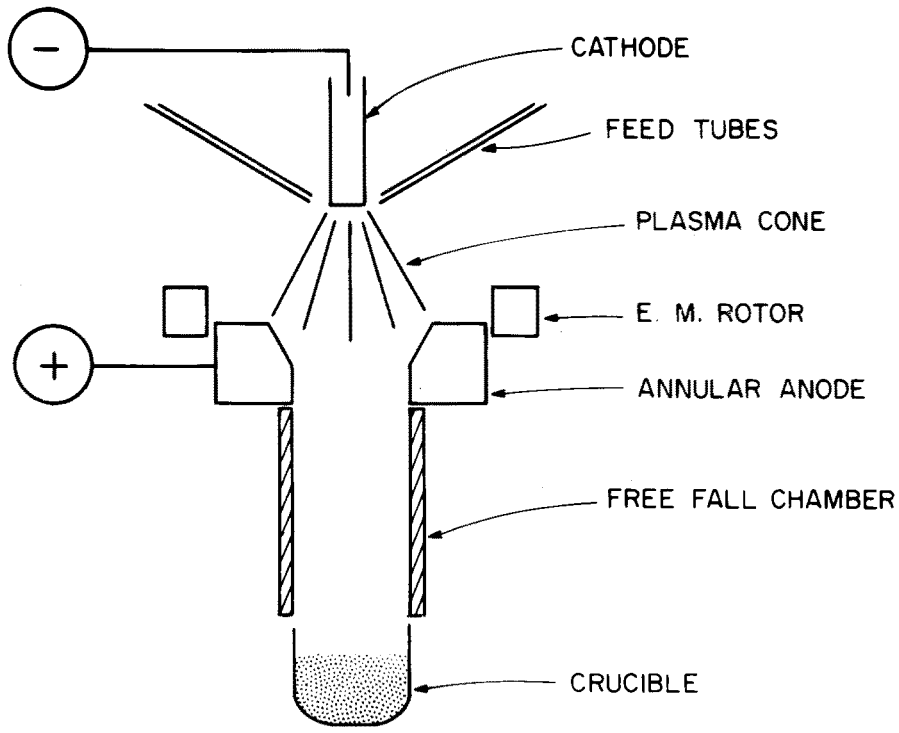

Figure 1 Schematic representation of the d.c. transferred arc plasma reactor and operating parameters. Expanded plasma arc cone: diameter at top of cone 20 mm, diameter at bottom of cone 90 mm, length of cone 90 mm, arc voltage 140 to 220 V, arc current 400 to 290 A, arc rotation 2000 to 10 000 r.p.m. Plasma gas: argon flow rate 0.8 $m^3 h^{-1}$.

magnetite concentrate and complex iron–chromium carbides from the chromite concentrate. The advantage of using these two systems is that the microstructure of these two systems is well documented.

The stoichiometry used for these two reactions was as given below i.e.

$$(FeO \cdot Cr_2O_3) + 17C = Fe_3C + 2Cr_3C_2 + 12CO$$

and

$$Fe_3O_4 + 4C = 3Fe + 4CO$$

and was based on the thermodynamic considerations discussed earlier. Using the experience gained from previous investigations of carbothermic reduction in a similar plasma environment [8, 9], a 200% stoichiometric carbon level of the above reactions was used in order to achieve maximum reduction of each oxide concentrate.

As can be seen from Table I, the level of silica impurity in both concentrates was approximately 6%. The stoichiometry of the reactants was varied in order to provide different yields of reduction. Fig. 3 indicates the level of reduction to metallic ion as a function of percentage reduction of Fe^{3+} to Fe^{2+} for the magnetite concentrate. With respect to the latter, the Fe^{2+} could be present as either FeO or metallic iron. As can be seen from Fig. 3, no metallization was achieved until 30% of the Fe^{3+} had been reduced to the Fe^{2+}, while the amount of Fe^{2+} remaining as FeO remained constant at approximately 30%. The

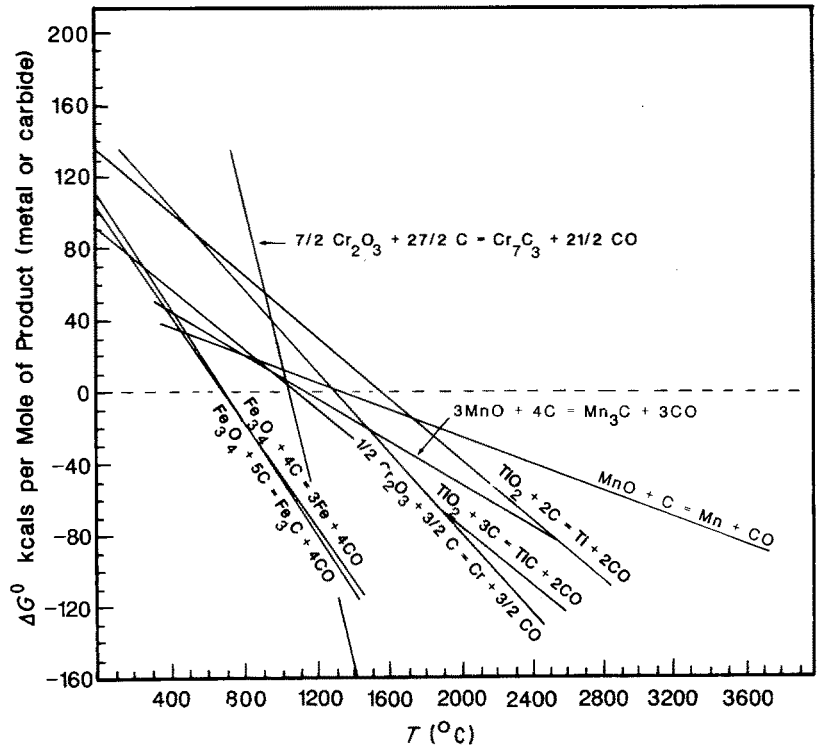

Figure 2 Plot of $\Delta G°$ against T.

TABLE I Chemical analyses of magnetite and chromite concentrates

Total Fe, Fe_T (%)	66.81	SiO_2 (%)	6.6
Fe^{3+} (%)	44.49	Al_2O_3 (%)	15.49
Fe^{2+} (%)	22.16	FeO (%)	21.3
FeO (%)	28.5	Fe_2O_3 (%)	1.6
Fe_2O_3 (%)	63.6	MgO (%)	15.25
Fe_3O_4 (%)	92.1	Cr_2O_3 (%)	38.95
Metallic Fe (%)	0.16	Na_2O (%)	0.20
SiO_2 (%)	6.23	K_2O	0.01
S (%)	0.004	TiO_2 (%)	0.41
		CaO (%)	0.51
		S (%)	0.021
		P (%)	0.011
		Cr/Fe	1.51

TABLE II Screen analysis of the magnetite and chromite concentrates

Mesh	Size (μm)	Taconite (wt %)	Chromite (wt %)
48	300	0.00	0.00
−48 + 65	−300 + 200	0.00	25.44
−65 + 100	−210 + 149	0.00	29.46
−100 + 150	−149 + 105	0.77	18.54
−150 + 200	−105 + 74	2.72	9.79
−200 + 270	−74 + 53	7.88	5.59
−270 + 325	−53 + 44	11.34	2.74
−325	−44	77.29	8.44
Total		100.00	100.00

maximum reduction of the oxide concentrate achieved was approximately 75% for the magnetite and approximately 65% FeO and 55% Cr_2O_3 for the chromite concentrate.

Table III gives the plasma product chemistries achieved with both magnetite and chromite concentrates operating under optimum plasma reduction conditions. Typical photomicrographs of the reduced products from the magnetite and chromite concentrates are given in Figs 4 and 5. From Fig. 4 it can be seen that the product is essentially a high carbon iron consisting of eutectic carbide (Fe_3C) and pearlite.

Measurement of the secondary dendrite arm spacing, λ_2, was made on the Fe_3O_4 reacted product in order to establish the average cooling rate and was found to be approximately 2.5 μm. Incorporating this value into the established relationship

$$\lambda_2 = a\varepsilon^{-n}$$

where constants, a and n, for a high carbon steel have been reported [10] as 70 and 0.42 respectively, provided an average cooling rate, ε, of $3 \times 10^3\,K\,sec^{-1}$. Measurement of the interlamellar spacing of the pearlite in this structure also provided a means of calculating the degree of supercooling for the eutectoid reaction [11] that occurred, (Fig. 6), and again an indication of metastability. The interlamellar spacing for this particular pearlite was determined to be 0.1 μm. This indicated an eutectoid transformation temperature of approximately 550 to 600° C, and undercooling of approximately 180° C.

The larger chromite particles provided a lower degree of reduction than the magnetite particles. At the same time the larger chromite particles allowed certain observations to be made which were not apparent with the smaller magnetite particles. Such important observations are provided in Fig. 5. It is seen that an essentially unreduced chromite particle has certain lines of preferentially reduced iron–chromium–carbide particles associated within it and that these fine reduced particles can coalesce into larger ones provided, presumably, that there is sufficient residence time in the plasma. The etched sample shown in the photomicrograph (Fig. 5b), shows that the primary phase is indeed a carbide. Examination of these larger plasma-processed chromite particles indicated that a low melting point slag phases, rich in magnesium silicate, was produced together with partially reduced chromite. The iron–chromium–carbon particles in this microstructure tended to be associated with the lower melting point magnesium silicate rich phase, which appears dark in the photomicrograph in Fig. 5a.

The SAM analysis of the phases present in the magnetite and chromite reduced particles is given in Table III.

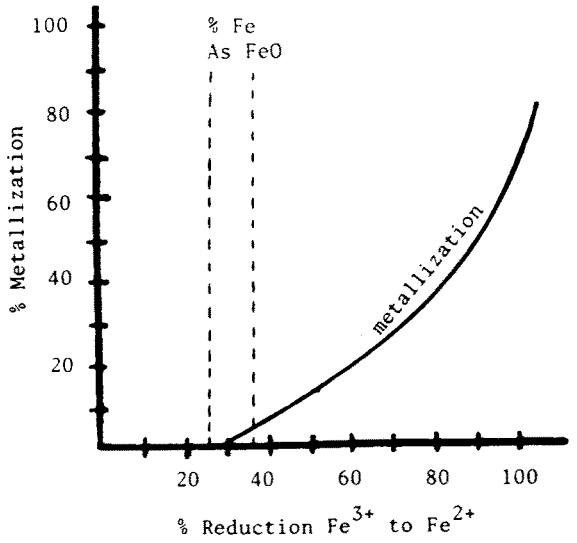

Figure 3 The reduction of metallic iron as a function of percentage reduction of Fe^{3+} to Fe^{2+} for the magnetite concentrate.

5. Discussion

The reaction mechanisms pertinent to this type of plasma reaction medium have been discussed in earlier papers [12–14] and are briefly outlined here. Initially, the very fine particles which are capable of melting and dissociating do so, thereby establishing a mixture of atoms of the elements of the reactants. Subsequent ionization of these atoms takes place to some degree. The selective reduction or removal of oxygen from these mineral oxides with carbon then takes place according to their thermodynamic stability, e.g. in the order FeO, Cr_2O_3, MgO, Al_2O_3.

From the thermodynamic considerations [2], it appears that iron oxide and chromium oxide are relatively easy to reduce, but the more stable oxides present in the mineral concentrates, e.g. MgO, Al_2O_3, SiO_2, require a much higher reduction potential within the plasma medium.

Magnetite, Fe_3O_4, can be represented as a spinel, $FeO \cdot Fe_2O_3$, and is reduced in two stages. The first

TABLE III SAM point analysis of plasma-produced particles (using internal standards)

Specimen	Phase		Fe (wt %)	C (wt %)	Cr (wt %)
Typical Particles produced from					
plasma-processed magnetite (Fe_3O_4)		From	98.2	1.8	
(maximum reduction: approx 75%)		To	96.2	3.8	
Typical phase analysis (Fe_3C (eutectic))				5.1	
(Pearlite)				1.8	
Typical Particles produced from					
plasma-processed chromite ($FeO \cdot Cr_2O_3$)			55.2	12.8	32.0
Maximum reduction: approx. 65% FeO					
55% Cr_2O_3					

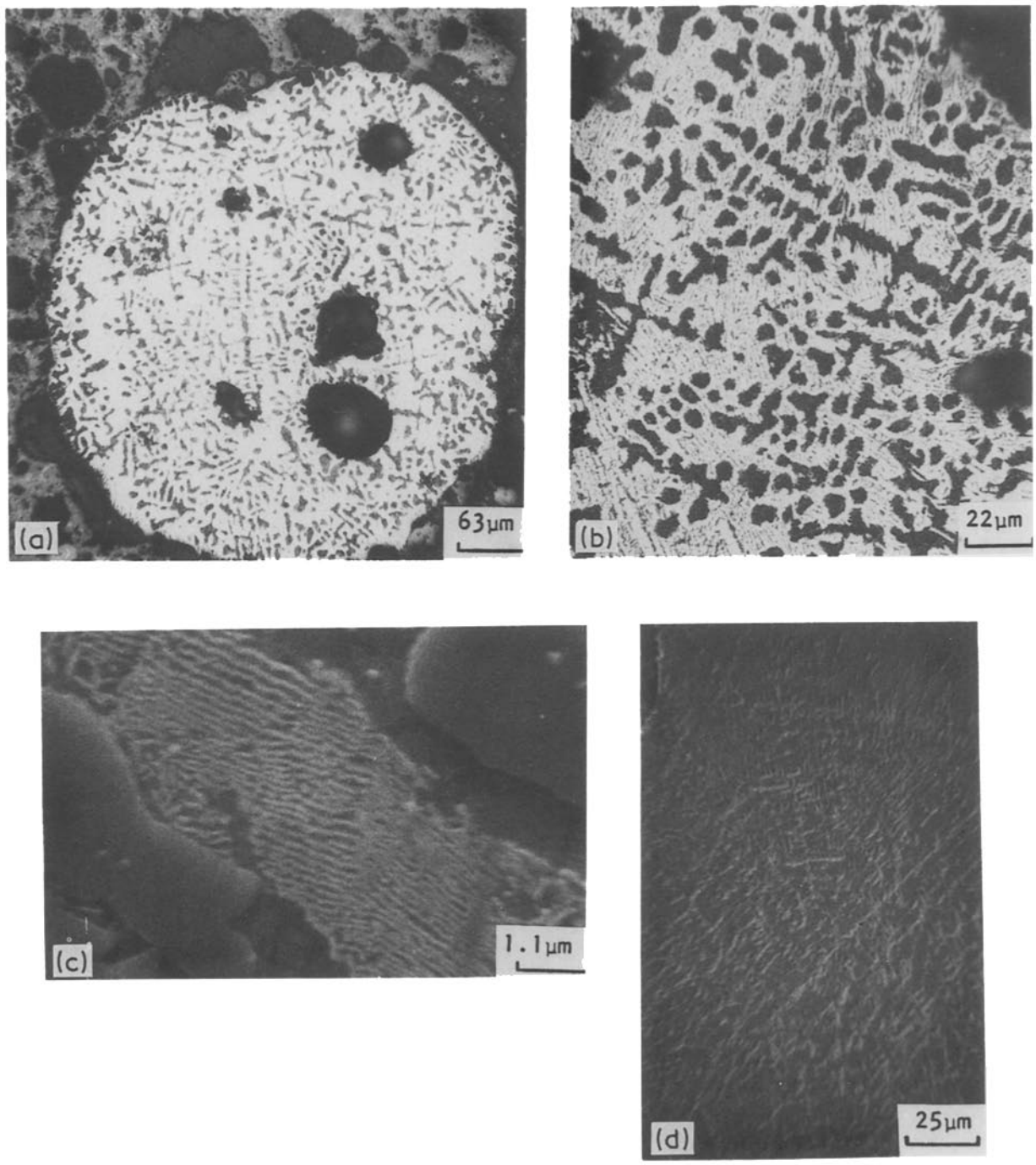

Figure 4 Scanning electron photomicrographs of a typical product from the carbothermic reduction of magnetite in the plasma reactor (etched in nital). (a), (b) iron–carbon particle surrounded by FeO–SiO_2 slag. Note: Structure in (b) is pearlite (dark) and eutectic Fe_3C (light). (c) Interlamellar spacing of the pearlite in (b). (d) Dendritic etch used on (b).

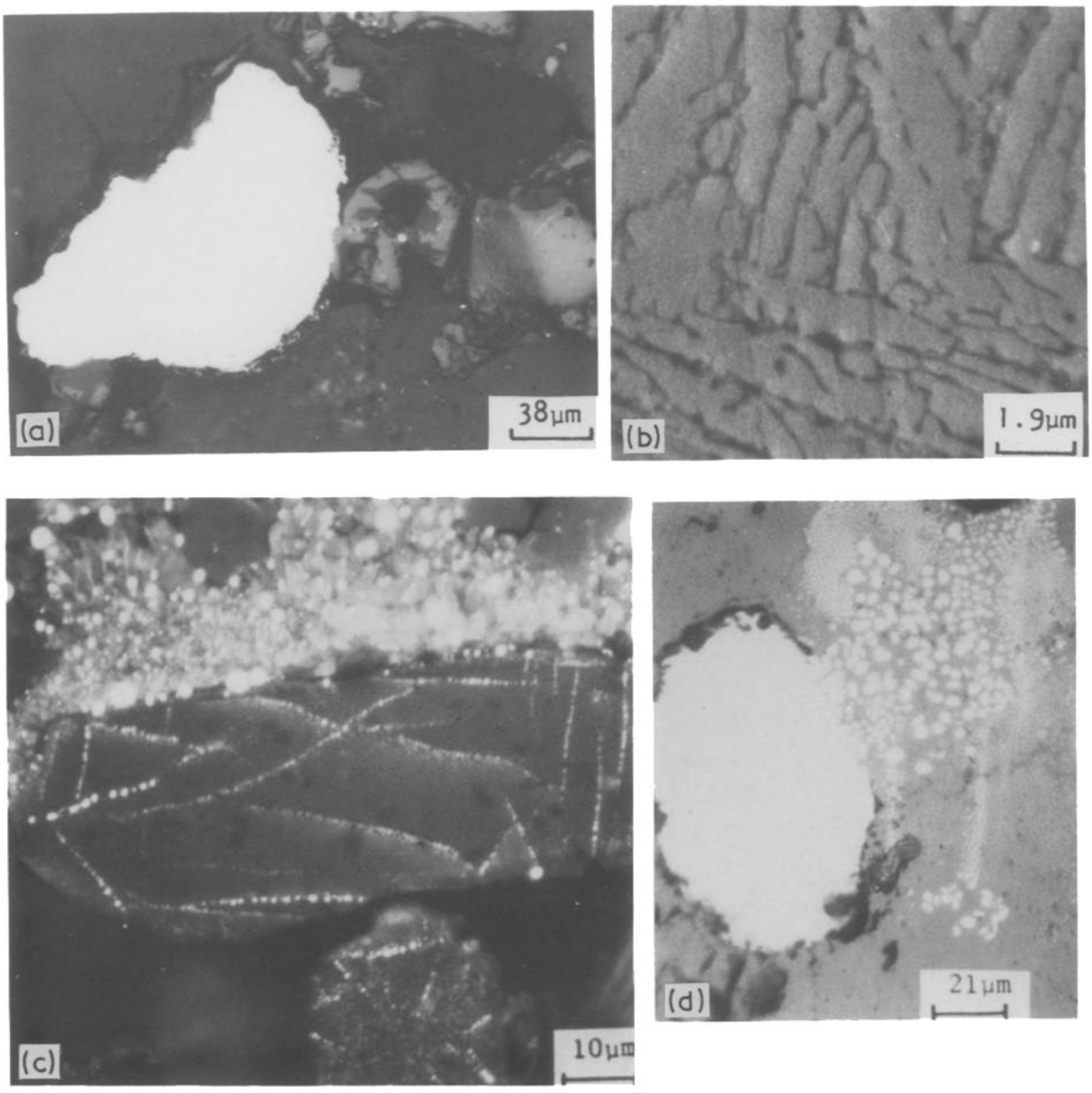

Figure 5 Scanning electron photomicrographs of typical products from the carbothermic reduction of chromite in the plasma reactor. (a), (b) iron–chromium–carbon particle surrounded by Mg_2SiO_4-rich slag. Note: high volume fraction of primary carbides in etch specimen in (b). (c) Unmelted chromite particles showing fine reduced (white) Fe–Cr–C particles situated along certain lines in the particle. (d) Coalescence of the fine iron–chromium–carbon particles in the Mg_2SiO_4 slag phase.

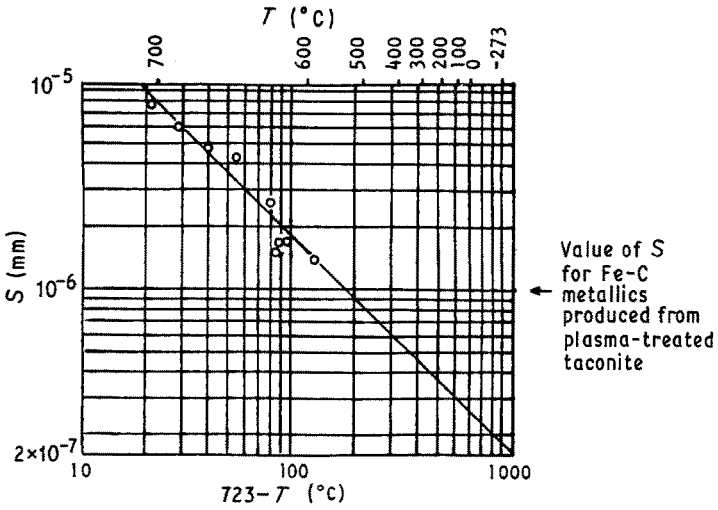

Figure 6 Variation of interlamellar spacing with undercooling. The open circles are experimentally determined values, the line is the relationship for S based on

$$S = \frac{4\sigma V_m}{\Delta H_m} \frac{T_0}{T_0 - T}$$

where σ is the specific surface energy for $\gamma \rightarrow$ pearlite reaction, V_m the molar volume of the material, ΔH_m the heat of transformation, T_0 the equilibrium eutectoid transformation temperature and $T_0 - T$ the degree of supercooling.

stage being the reduction of any Fe^{3+} present to FeO, e.g.

$$FeO \cdot Fe_2O_3 + C = 3FeO + CO;$$

and the second stage being the more energetically demanding FeO reduction, i.e.

$$FeO + C = Fe + CO.$$

However, unlike conventional direct reduction of Fe_2O_3 [3–7], this second reduction stage appears to start before completion of the Fe_2O_3 reduction to FeO in the plasma medium. The presence of slag forming constituents, e.g. SiO_2, complicates the issue by forming silicates, e.g. $FeO \cdot SiO_2$. This was confirmed by electron microprobe analysis. Such silicate formation reduces the activity of FeO making the reduction of FeO to Fe thermodynamically more difficulty. Conducting a material balance on the magnetite system it was apparent that 30% reduction of Fe^{3+} to Fe^{2+} remained as FeO in the form of $FeO \cdot SiO_2$, and in this condition, under the reduction potential prevailing in this plasma reactor, the activity of FeO was too low to effect reduction.

The smaller magnetite particles were completely melted within the plasma medium as evidenced by the fact that the products in every case appeared spherical. However, the larger sized chromite particles in some areas retained their angularity (Fig. 5c) and, therefore, have not melted or, at best, only partially melted. Such observations of the chromite reduced products indicates that partial melting and partial reduction has therefore taken place. A typical example is given in Fig. 5c in which the large chromite particle is essentially unmelted, but reduction has taken place along certain preferred internal channels within the chromite particle and manifested in the form of very fine iron–chromium–carbon particles. The composition of these iron–chromium–carbon particles ranged from iron–carbon metallics with no chromium, similar to those produced from the magnetite concentrate (Fig. 4), to those with iron to chromium ratio of 1 : 1 with up to 13% carbon present. This is probably due to the highly variable reduction conditions existing within the plasma medium, the kinetic dependence of these reactions with very short plasma residence times, particle size and particle chemistry.

The association of the reduced iron–chromium–carbon particles in the low melting point magnesium silicate rich phase can be explained in that the partial melting of the chromite particles resulted in the formation of low melting point constituents such as Mg_2SiO_4 which can provide a liquid medium in which the reduction reactions may proceed.

The iron–chromium–carbon particles present in the unreduced chromite mineral appeared to be present along certain crystalline boundaries within the mineral crystal. One possible explanation for this is that the mineral particle, on being subjected to the plasma conditions, is ripped apart and any volatiles that are present travel along these very fine channels, essentially producing a channel of plasma. This channel is highly reducing and provides an active path along which reduction can be initiated. These observations, although speculative indicate the importance of particle size and mineral chemistry when endeavouring to effect maximum plasma–particle interaction.

The very high carbon level obtained in the products indicates high reaction temperatures and rapid solidification rates. At the high reaction temperatures achieved in this plasma, i.e. maximum temperatures measured using spectroscopic techniques were approximately 8000 K, carbon diffusion rates are extremely high and give rise to total saturation with carbon. This, coupled with rapid solidification through the liquid–solid phase transformation, provides an extremely high carbon level over and above that for the equilibrium phase. Examination of the phases obtained in the SAM analysis indicated an eutectic carbide containing only approximately 5% carbon while the pearlite contained approximately 1.8% carbon. It appears, therefore, that the pro-eutectic γ which subsequently transformed to pearlite was supersaturated with carbon due to the rapid cooling rate of $10^3\,K\,sec^{-1}$. This resulted in a lower than equilibrium level of carbon for the subsequent formation of eutectic carbide. Although these analyses using the SAM are, at best, only indicative since they use internal standards rather than external standards, they do provide a general guide as to the degree of metastability. This degree of metastability is also supported by measurements of the secondary dendrite arm spacing and the corresponding calculation of the average cooling rate that can occur when particles exit the plasma medium and enter the ambient atmosphere. Also coupled with this would be the inter-lamellar spacing determination and calculation of the super cooling of the eutectoid reaction. A solidification rate of $10^3\,K\,sec^{-1}$ does not closely correspond with a super cooling of the eutectoid reaction of approximately 180° C. This may be explained in that cooling from the liquid to solid state at a rate of $10^3\,K\,sec^{-1}$ can be readily achieved on leaving the plasma medium. However, the condensed phase tended to be associated with an envelope of liquid slag, e.g. $FeO \cdot SiO_2$ (magnetite), Mg_2SiO_4 (chromite), produced from the slag forming constituents present in the mineral concentrate. These will have a lower melting point and will, therefore, condense around the solid carbides (Figs 4a and 5a), substantially reducing the heat transfer. This will result in a lower cooling rate as the temperature approaches the eutectoid transformation for the Fe_3O_4–C system compared with that for the liquid to solid transformation.

6. Conclusions

Commercially available mineral concentrates of magnetite and chromite have been reduced in a plasma medium within 100 msec residence time. The degree of metallisation has been found to be dependent upon the mineral size and mineral chemistry and can be indicated from examination of thermodynamic and kinetic principles. The maximum reduction achieved with the 44 μm magnetite particle was approximately 75%, whereas that for the larger chromite particle was around 60%. Examination of the products using quantitative metallography and EDAX facilities on an

SEM together with elemental analysis using a SAM has indicated a high degree of metastability. This high degree of metastability is manifested in much higher carbon concentrations and finer dendritic and pearlitic structures than would be achieved under equilibrium conditions.

It is apparent that the presence of the slag forming constituents in a commercially available concentrate decreases the ability of the plasma medium to reduce the oxide, and, furthermore, decreases the degree of metastability due to the formation of a slag envelope around the reduced particles with a resultant lowering of the heat transfer rates and subsequent solid phase transformation rates.

Acknowledgements

The author wishes to thank Professor K. J. Reid, Director, Mineral Resources Research Center, University of Minnesota, for the provision of the research facilities.

References

1. J. J. MOORE, J. K. TYLKO, and K. J. REID, Proceedings Extractive Metallurgy of Refractory Metals, Chicago, Feb, 1981 edited by H. Y. Sohn and J. T. Smith (TMS-AIME) pp. 377–417.
2. K. UPADHYA, J. J. MOORE and K. J. REID, *Metall. Trans,* **17B** (1986) 192–207.
3. Y. K. RAO, *Metall. Trans.,* **2** (1971) 1439.
4. R. J. FRUEHAN, *Metall. Trans.* **8B** (1977) 279.
5. D. OTSUKA and D. KUNNI, *J. Chem. Eng. Jpn,* **2** (1969) 46.
6. Y. K. RAO, *Chem. Eng. Sci.* **29** (1974) 1435.
7. E. T. TURKDOGAN, R. J. FRUEHAN and J. K. TIER, Proceedings Darken Conference on Physical Chemistry in Metallurgy, United States Steel, Monroeville, PA, (1976) p. 166.
8. K. J. REID, J. K. TYLKO and J. J. MOORE, Second World Congress of Chemical Engineering, Montreal, Canada, October (1981) p. 1–11.
9. K. J. REID, J. J. MOORE and J. K. TYLKO, Proceedings 5th ISPC, IUPAC, Edinburgh, August (1981).
10. A. SUZUKI, T. SUZUKI. Y. NAGAOKA and Y. IWATA, *Nippon Kingaku Gakkai Shuho,* **32** (1968).
11. M. HILLERT, Proceedings of the Darken Conference on Physical Chemistry in Metallurgy, (US Steel, 1976) p. 445–462.
12. K. J. REID and J. J. MOORE, Proc. 54th Annual Minnesota Sec. AIME Meeting, Duluth, January 1981, (University of Minnesota, 1982) p. 12–1.
13. J. J. MOORE, K. J. REID and J. K. TYLKO, *J. Met.,* August (1981) p. 43.
14. K. J. REID, M. MURAWA and N. M. GIRGIS: Proceedings 6th International Symposium of Plasma Chemistry ISPC-6, Montreal, 1983.

Received 1 June
and accepted 21 October 1988